Measuring chaotic noise in nonlinear models

Michel Pitermann

INTERNATIONAL JOURNAL OF
INFORMATION AND SYSTEMS SCIENCES
Volume 5, Number 1, Pages 1–14

MEASURING CHAOTIC NOISE IN NONLINEAR MODELS

MICHEL PITERMANN

Abstract. In many applications such as fluid or solid modeling, chaotic noise may be cumbersome. Instead of estimating the Lyapunov exponent of the system, one may be interested in measuring the amplitude of the system's chaotic noise in a unit better suited to the application, e.g., the amplitude (in mm) of the vibration of a solid's surface. The goal of this study is to propose a method to achieve this goal. The techniques are tested on a nonlinear biomechanical model of the face driven by muscle activity and a jaw hinge. The proposed method is effective and shows that (i) the amplitude of chaotic noise perceivable as skin vibration is approximately equal to 10% of the amplitude of a full-scale movement; (ii) the noise properties are similar in the stationary and dynamic states; (iii) the noise comes only from the skin model, not from the nonlinear muscle models. The method is simple and inexpensive to implement. It can therefore be useful in applications such as video animation or motor control research, where estimating the component of chaotic noise is more important than fully characterizing the nonlinear properties of a model.

Key Words. chaotic noise, nonlinear modeling, biomechanical modeling, face model

1. Introduction

Chaos has been widely studied since the first publication on this issue [7]. In many fields, chaotic properties of nonlinear models are useful for matching system behavior. Some of these fields are epidemic modeling [13], fluid mechanics [2] and atmospheric modeling [14]. In other areas, nonlinear modeling is required to properly describe phenomena, but chaos acts as undesirable noise. For example, in fluid mechanics or in solid modeling, finite element methods are widely used [4], and the chaotic properties of the models may be difficult to handle [3]. In solid modeling, soft tissue may also be modeled by point masses connected by springs [15, 18, 6, 10]. In these cases, chaos produces a potentially visible vibration of the tissue. This poses a problem in computer animation because the skin of a real person that is immobile does not vibrate. Hence any chaotic vibration due to the nonlinear properties of the model must be invisible to spectators. A general method for quantifying chaotic noise is therefore required for these fields to decide whether the noise is acceptable or the model must be modified.

The Lyapunov exponent of a dynamic system described by a nonlinear model can be calculated, but it does not supply enough information about the visibility of its chaotic noise. A method that assesses the amplitude of the skin vibration due

Received by the editors April 12, 2007.
2000 *Mathematics Subject Classification.* 65P20,65G99.
This research was supported by NIH Grant from the National Institute of Deafness and other Communication Disorders and NSERC; contract/grant number: DC–00594.

to model chaos may therefore be preferred. The goal of this paper is to propose a method for quantifying the chaotic noise of nonlinear models in a unit that can be directly used in applications such as video animation. Instead of presenting the method in its most general and abstract form, the techniques will be detailed in a real example: a biomechanical model of the face, i.e., a model describing the physical properties of a human face. Firstly, the basic principle of the method will be presented; details will follow with the description of several computer simulations that test the method.

2. General method

The basic principle of the method can be broken down into three steps:

(1) An initial quantification of chaotic-noise amplitude, with the model in a stationary state without making statistical assumptions about the chaotic noise. This technique, which constitutes our stationary-state reference, cannot be used when the model is in a dynamic state. It therefore must be extended.
(2) A second estimation of chaotic-noise amplitude in a stationary state making a statistical assumption about the chaotic noise. This second estimate, which can be used when the model is in a dynamic state, must be compared to the previous one to validate the noise assumption.
(3) An estimation of chaotic-noise amplitude in the dynamic state using the second procedure if the noise assumption is correct.

As stated before, the techniques will be illustrated by analysing of a biomechanical model of the face. The common characteristics of all computer simulations will be described here, while their unique aspects will be outlined in separate sections.

2.1. The face model. A C++ program implementing the face model described in [8] was used in all experiments. Because this version of the model is thoroughly described in [8], its main characteristics will only be summarized here.

The model is composed of a jaw, a skin, and a muscle module. The jaw is simulated by a simple hinge kinematically controlled by adjusting the angle. The other two modules are more complex.

The skin was modeled by a deformable multi-layered mesh with isotropic mechanical characteristics. The 1435 nodes composing the mesh are point masses connected by approximately 6000 damped springs. The nodes are arranged in three layers representing the structure of facial tissues. The top layer corresponds to the epidermis, the middle layer the fascia, and the bottom layer follows the skull's surface. The elements between the top and middle layers represent the dermal-fatty tissue, and the elements between the middle and bottom layers represent the muscle tissues. The skull nodes are fixed in three-dimensional space. The fascia nodes are connected to the skull layer except in the region around the upper and lower lips and the cheeks. The epidermal layer is shown in green in Fig. 1a. A piecewise linear biphasic approximation was used for dermal-fatty spring force elongation, and a linear approximation was used for all other spring force elongations. A nonlinear approximation was used for spring force compression to provide infinite growth of the force as spring length approaches zero.

The muscles were modeled using a standard Hill-type formula that constrains force generation due to the contractile element (a force depending on muscle length variation and velocity) and a static dependence of force on muscle length [20, 19, 5]. Standard skeletal muscle physiology was assumed and the muscles are represented

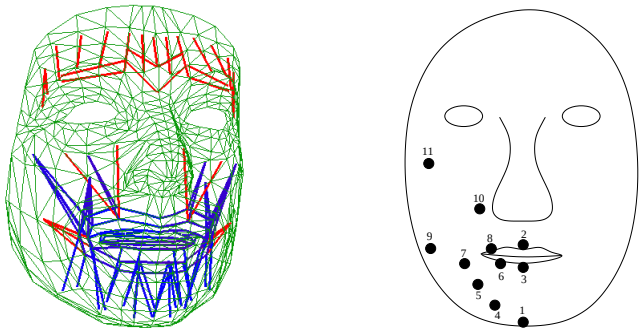

a) b)

FIGURE 1. a) Lines of action of the modeled muscles in red and blue, printed over the mesh corresponding to the skin surface in green. The muscles printed in blue were activated during the experiments; the other ones were not. b) Approximate positions and numbering of the analyzed nodes (black spots).

as linear force vectors. Thus, the force applied by a modeled muscle to its connected nodes could be calculated from its activity level (its electrochemical potential) using the Hill-type formula.

The morphology of the model was adapted to the speaker's morphology to enhance model naturalness. ATR Human Information Processing Research Laboratories, Kyoto, Japan, owns this data and kindly offered to let me use it.

The general equation for the motion of each node i of the model is [15, 6, 8]:

$$m\frac{\mathrm{d}^2 x_i}{\mathrm{d}t^2} + r\sum_j \left(\frac{\mathrm{d}x_i}{\mathrm{d}t} - \frac{\mathrm{d}x_j}{\mathrm{d}t}\right) + \sum_j g_{ij} + \sum_e q_i^e + s_i + h_i = F_i \tag{1}$$

where x_i is the current position of node i, m is the node mass equal to 0.00023 kg per node, the second term of the sum is the total damping force acting on node i (x_j represents the nodes connected to node i, and r is a constant equal to 0.050 kg/s), g_{ij} is the spring force applied by node j to node i, the fourth term models skin incompressibility (q_i^e represents the triangular prism elements containing node i), the fifth term s_i is the skull's reaction to the force applied by the fascia nodes, the sixth term h_i is a nodal restoration force applied to the fascia nodes connected to the skull, and F_i is the total muscle force applied to node i. The terms g_{ij}, q_i^e, and h_i are the nonlinear components of the model. Details can be found in [15, 6, 8].

2.2. Animation. In all analyses, the same eight pairs of muscles (a pair being made up of one muscle on each side of the face) as those used in [8] were synchronously activated using the same electrochemical potential for each muscle. The eight muscle pairs were the levator labii superior, levator anguli oris, zygomatic major, depressor anguli oris, depressor labii inferior, mentalis, orbicularis oris superior, and orbicularis oris inferior (see Fig. 1a). To avoid perturbation due to lip contact and jaw movement, the jaw angle was held constant at 2 degrees, which kept the lips apart in all simulations. The experiments were also carried out for jaw angles allowing lip contact, but because the conclusions were always the same, only the former results are reported here.

To animate the model, one frame was computed every 1/60 s. The motion equation (1) was solved using a classical fourth-order Runge-Kutta formula with a constant step in 50 iterations [12, section 16.1]. The muscle force was considered constant during each frame period, and the previous, computed frame was the initial condition of the Runge-Kutta algorithm for the current frame. All animations started with null muscle activity so that the resting position of the face could be used as the first initial condition.

The standard Runge-Kutta algorithm may be unstable when the step is too big. For example, using 50 iterations only worked for low muscle activity. As soon as the electrochemical potential of a muscle increased, between 100 and 500 iterations were needed. The relationship between muscle activity and requested number of steps seemed rather complex. Instead of carrying out a full sensitivity analysis to understand that relationship, an instability detector was added to the basic algorithm. When the algorithm was found to be unstable, the step size was divided by 2 and stability was checked again until convergence.

2.3. Statistical analyses. To statistically analyze skin vibration, the 3D trajectories of the same 11 points in the face model studied in [8] were tracked. Their approximate positions are shown as 11 numbered black spots in Fig. 1b.

A few one-dimensional (1D) statistical features were generalized in three dimensions to characterize the 3D node trajectories. The mean position of a 3D node trajectory v composed of n samples (x_i, y_i, z_i) was its centroid μ_v:

$$\mu_v = \left(\frac{1}{n} \sum_{i=1}^{n} x_i, \frac{1}{n} \sum_{i=1}^{n} y_i, \frac{1}{n} \sum_{i=1}^{n} z_i \right) \tag{2}$$

The standard deviation σ_v of a 3D node trajectory v was estimated by:

$$\sigma_v = \sqrt{\frac{1}{n-1} \sum_{i=1}^{n} |v_i|^2 - |\mu_v|^2} \tag{3}$$

where $||^2$ is the square magnitude operator of a vector, i.e., $|v_i|^2 = x_i^2 + y_i^2 + z_i^2$. The standard deviation of a node trajectory was used as the estimate of the 3D dispersion of the node around its mean position. The 3D correlation ρ_{vw} between two node trajectories v and w composed of n v_i samples and n w_i samples was:

$$\rho_{vw} = \frac{\frac{1}{n} \sum_{i=1}^{n} v_i.w_i - \mu_v.\mu_w}{\sigma_v \sigma_w} \tag{4}$$

where the dot in $v_i.w_i$ and $\mu_v.\mu_w$ is the dot product of two vectors. Like a 1D correlation, ρ_{vw} always belongs to the interval $[-1, 1]$. The difference between two time series v and w was defined by:

$$\Delta_{vw} = v_i - w_i \qquad \forall i \tag{5}$$

where i is any time coordinate in the time series. Finally, a few two-way analyses of variance were carried out to test the hypothesis that various factors had no influence on the statistical estimators. A rejection level of 0.05 was always used.

3. Experiment 1: Stationary state without noise assumptions

As explained in Section 2, the goal of the first set of simulations was to produce an estimate of the chaotic-noise amplitude in the stationary state, to be used as a reference. In the face model, this meant assessing the model's intrinsic skin-vibration amplitude component and comparing that estimate to the amplitude of

an extreme face movement produced with the model in a stationary state, i.e., for constant muscle activity.

3.1. Method. The sixteen selected muscles were synchronously activated by a step function composed of 10 samples set to 0, followed by 1400 samples set to 1. Then the resulting movement amplitude and skin vibration amplitude were measured and compared. A value of 0 corresponded to no muscle activity. The value 1 was chosen because in [8], facial muscle activity was measured for a speaker producing speech material and a set of extreme facial gestures. The electrochemical potentials of the muscle models were all normalized by the highest levels recorded in the corpus. A value of 1 was therefore considered as the maximum activity level a muscle could reach.

A node's movement amplitude was estimated as the Euclidean distance between the node's mean position when the muscles were maximally activated and the node's mean position when the muscles received a null input. To estimate the mean position of a node when the muscles were maximally activated, the impulse response of each node was studied and found to be shorter than 60 frames (1 s). Hence, the face model had always reached an equilibrium after the first 200 samples (3.33 s) of an animation resulting from the step function. Accordingly, the mean position of a node was estimated by the mean of its 3D node trajectory [Eq. (2)] computed over the last 1200 frames of the step function. Similarly, the node's resting position was estimated by its 3D trajectory mean when the face was driven by a null input composed of 1200 frames.

Skin-vibration amplitude was estimated by the 3D standard deviation [Eq. (3)] of each node trajectory. The 3D standard deviations were computed over the last 1200 frames of the step function, i.e., when the face model was in equilibrium with its muscle activity set at its maximum. All calculations were made three times, each time with a different computing precision: single, double, and quadruple precision corresponding, to the C++ types "float", "double", and "long double". These types corresponded to 32-, 64-, and 128-bit floating-point representations in the C++ implementation used (gcc 2.95.2 on an UltraSparc II running Solaris 2.7).

3.2. Results and discussion. Fig. 2 presents different estimates of the standard deviations of 11 nodes of the face model after it had reached an equilibrium in a stationary state. The results of the first set of simulations are shown by the three lines labeled Simplem, Double, and Quadr. Since the output of the model was expected to be constant after reaching an equilibrium, any new movement was considered as undesirable skin vibration. Fig. 2 data thus corresponds to the measures of the average amplitude of skin vibration in different areas of the face.

The three lines of the graph labeled Simple, Double, and Quadr. correspond to 3D standard deviations of node trajectories when the face movements were computed in single, double, or quadruple precision during the stable part of the step function. A two-way ("node position" and "computing accuracy") analysis of variance on the standard deviations yielded significant effect (at the 0.05 level) of node position [$F(10, 20) = 175.33, p < 1e - 9$] but not computing accuracy [$F(2, 20) = 1.22, p = 0.32$]. This means that skin-vibration amplitude was different in different areas of the face, but no dependence of skin vibration on computing accuracy was found. As a consequence, the amplitude of this undesirable "noise" could not be decreased by improving the precision of the calculations. This noise therefore stems from the chaos properties of the face model.

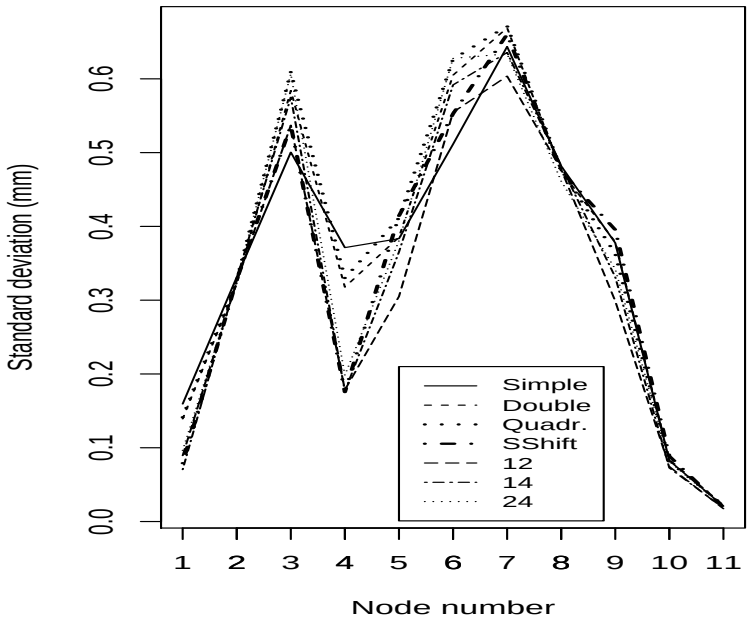

FIGURE 2. Estimates of skin-vibration amplitude, by node number (see Fig. 1b for the position of each node on the face) when the face model was in a stationary state with 16 muscle activations set at their maximum. The first three labels of the legend mean that the face model calculations were carried out in single, double, or quadruple precision. SShift means that each node vibration amplitude was estimated by taking the difference between two corresponding node trajectories computed with the same muscle activity, but node 3 was shifted by 0.001 mm to the right on the tenth frame (the first S stands for Static). The three labels 12, 14, and 24 mean that each standard deviation was estimated by means of the difference between two corresponding node trajectories computed with the same muscle activity and the same initial condition, but using different computing precisions (1 for single, 2 for double, and 4 for quadruple), e.g., 14 means single minus quadruple precision.

Skin-vibration amplitude was compared to face-movement amplitude. Fig. 3 presents the results when the face was animated by the step function. This figure and Fig. 2 indicate that the ratio of the resulting face movement to the skin-vibration amplitude was approximately 10:1 (compare the y scales). Hence, skin vibration did not override facial movements, although it was not negligible.

4. Experiment 2: Stationary state with a noise assumption

Studying the chaotic noise of a model in a dynamic state (control parameters varying over time) cannot be done using 3D standard deviations of the model output. Such standard deviations would contain a noise component and a component due to movements resulting from variations in the control parameters. So, a means of getting rid of the control-parameter component had to be used. Experiment 2

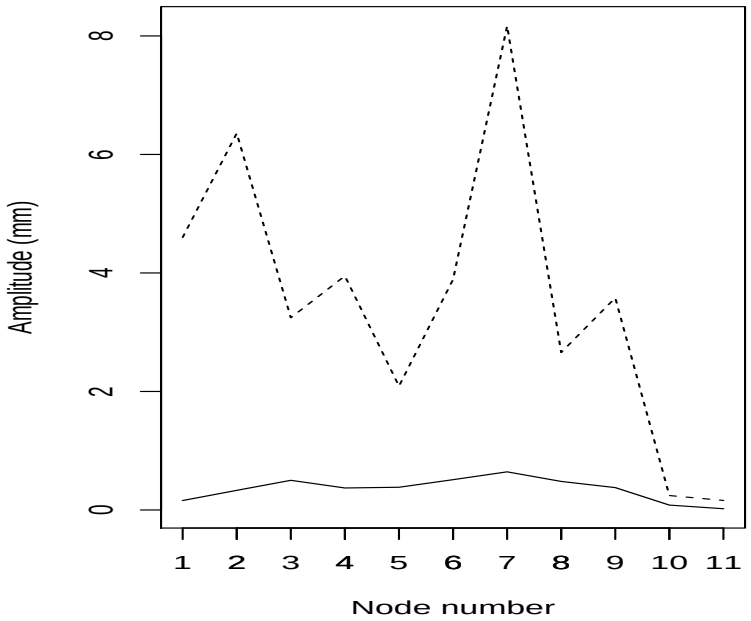

FIGURE 3. Amplitude of a face movement (dashed line) and skin vibration (solid line) for different areas of the face model, by node number (see Fig. 1b for the position of each node on the face) when sixteen modeled muscles were activated by a step function. The solid line corresponds to the solid line in Fig. 2.

was designed to test such a technique. The results produced in this new experiment then had to be compared to the initial results of Experiment 1 taken as the stationary-state reference. If the two techniques agreed, the new procedure would be used for a dynamic state.

The results of the previous set of simulations showed that the face model suffered from chaotic noise. With this model, any given simulation in a stationary state would produce an output v that seems to fluctuate erraticlly around a fixed value. The output v might therefore be considered as a pseudo-random variable. Another simulation with the same control parameters but with different initial conditions would lead to a similar model output, w, also characterized by erratic behavior around the same fixed value. Output w might therefore also be considered as a pseudo-random variable. If the two initial conditions are very close, the difference Δ_{vw} (Eq. 5) will be close to $(0, 0, 0)$ at the beginning of the simulation. Then the magnitude of Δ_{vw} will increase exponentially over time due to sensitivity to the initial conditions, until Δ_{vw} begins to vary erratically around a fixed value. In other words, v and w will seem to be two independent pseudo-random variables characterized by the same mean and the same variance. The variance of the corresponding Δ_{vw} should therefore be the sum of the variances of the two independent random variables. Hence, the variance of Δ_{vw} should be equal to twice the variance of v or w. So, the amplitude of the chaotic noise of a model could be estimated by carrying out two simulations with the same control parameter values but two different initial conditions. The variance of the difference Δ_{vw} between the two output trajectories v and w should be equal to twice the variance component of v

or w due to chaotic noise. Thus, the standard deviation of Δ_{vw} should be divided by $\sqrt{2}$ to estimate the amplitude of the chaotic noise.

In the same way, performing the calculations of a simulation with two different computing accuracy levels should lead to two slightly different simulations, because of different roundoff errors. With sensitivity to initial conditions, the small differences due to roundoff error can be expected to increase exponentially over time. Therefore, calculating Δ_{vw} for two simulations characterized by two different initial conditions or two different computing accuracy levels should lead to two similar variances that are approximately equal to twice the variance estimated in the previous experiment. The purpose of this experiment was to test this hypothesis on the face model.

4.1. Method. The same step function composed of 10 samples set at 0, followed by 1400 samples set at 1, was used to synchronously activate the 16 selected muscles. To work with two different initial conditions, the initial condition chosen in the previous experiment was used again except that node 3 was shifted to the right by 0.001 mm on the tenth frame, i.e., just before muscle activation. Single precision was used in the calculations. For each node, the difference Δ_{vw} between the new trajectory and the one calculated in single precision during the first experiment was computed.

The simulations were carried out for three computing accuracy levels in the first experiment. For each node, the difference Δ_{vw} was also computed for each pair of trajectories computed with the same muscle activity and initial conditions but with two different precisions.

The 3D standard deviation of each Δ_{vw} was computed over the last 1200 frames of the step function, i.e., when the face model was in equilibrium with its muscle activity set at its maximum. All standard deviations were divided by $\sqrt{2}$.

4.2. Results and discussion. Fig. 2 presents the different standard-deviations estimates of 11 nodes in the face model after it had reached a stationary state. The three lines labeled Simple, Double, and Quadr. are discussed above in Section 3.2 about the first experiment. The line labeled SShift corresponds to the results of the simulation using the same muscle activity but two different initial conditions. In this case, node 3 was shifted to the right by 0.001 mm on the tenth frame, i.e., just before the step in the input. Hence, the only difference on the tenth frame between the faces in the first and new simulations was the 3D position of one node (out of 1435) shifted by 0.001 mm. This small difference increased exponentially over time and was propagated throughout the entire mesh. As explained above, it was assumed that the node trajectories of the new simulation would be independent of the old ones when the face model had reached its equilibrium. The first row of Table 1 shows that this assumption was not always true. The table presents the 3D correlations between pairs of node trajectories, computed with the same muscle activity but different initial conditions or computing precisions. All correlations were measured for the last 1200 frames of the 1410-frame step functions. Based on the first row of the table, it seems that some the 3D correlations between new and old node trajectories are high (especially nodes 1 and 4). The independence assumption was nevertheless taken as a first approximation, with the difference between the old and new trajectories [Eq. (5)] being used to calculate a new estimate of the average skin-vibration amplitude. Fig. 2 shows that the match between this new estimate and those produced in Experiment 1 is good (line labeled SShift compared to Simple, Double, and Quadr.)

TABLE 1. 3D correlations [Eq. (4)] in a stationary state (Experiment 2) between pairs of node trajectories computed at two different precision levels (1, 2, and 4 for single, double, and quadruple precision, respectively), or between pairs of node trajectories computed in single precision but with different initial conditions (SShift row). The sole difference between the two initial conditions was the position of node 3, which was shifted 0.001 mm to the right on the tenth frame. Each column of the table presents the correlations for a different node (see Fig. 1 for the correspondence between node number and node position on the face).

	Node Position										
	1	2	3	4	5	6	7	8	9	10	11
SShift	0.72	-0.02	0.01	0.75	-0.07	0.01	0.00	0.04	-0.13	-0.20	0.06
1–2	0.65	0.01	0.02	0.74	0.37	0.02	0.15	0.00	0.38	0.20	0.36
1–4	0.79	0.00	-0.06	0.75	0.16	-0.07	0.07	-0.01	0.20	0.21	0.28
2–4	0.53	0.00	-0.03	0.63	0.09	-0.04	0.11	0.06	0.15	0.03	0.24

In the same way, carrying out the calculations of a simulation with two different computing precisions should lead to similar results because of the different round-off errors and sensitivity to initial conditions. The results are reported in Fig. 2 where one can see that using two different initial conditions or computing precisions produced similar results (lines labeled SShift compared to 12, 14, and 24).

Finally, Fig. 2 shows that estimating skin-vibration amplitude by means of 3D standard deviations of node trajectories when the model is in a stationary state, or by means of 3D standard deviations of differences between pairs of node trajectories divided by $\sqrt{2}$, produces similar results (lines labeled Simple, Double, and Quadr. compared to the other four lines). A two-way ("node position" and "method" of estimating skin-vibration amplitude, i.e., with or without the trajectory difference) analysis of variance on the estimates of skin vibration amplitude yielded a significant effect (at the 0.05 level) of node position $[F(10, 55) = 468.87, p < 1e - 9]$, method $[F(1, 55) = 23.55, p < 2e - 4]$, and an interaction between these two factors $[F(10, 55) = 5.62, p < 1e - 05]$. As Fig. 2 indicates, the results produced by all methods were so close that they can be considered identical for all practical purposes. This is important for the next experiment, which used time-varying muscle activity, because only methods based on differences between pairs of trajectories will be applicable.

4.3. Conclusion for the stationary state. To summarize the results so far, the face model was found to be sensitive to initial conditions and generated skin vibration that was independent of computing accuracy. The average skin-vibration amplitude was firstly estimated using the 3D standard deviation [Eq. (3)] of each node position when the model was animated by constant muscle activity. No assumption about noise was made for the first estimate. Because this method could not be used in a dynamic state, another technique involving differences between pairs of trajectories was also implemented. These differences could potentially eliminate the component of face movement due to variations in the control parameters over time, but it required the assumption that two trajectories differing only by chaotic noise could be considered as two independent variables once the control-parameter variation was factored out. This second approach produced results so close to the first ones (the reference) that the two techniques can be considered equivalent for

all practical purposes. As a consequence, the simulations can also be carried out for a dynamic state.

5. Experiment 3: Dynamic state

After studying the face model in the stationary state, the analysis was replicated in the dynamic state (fluctuating muscle activity). Would new properties emerge from the dynamic state?

5.1. Method. The same sixteen muscles were synchronously excited by a wave of triangular activity composed of the sequence (0, 1/6, 2/6, 3/6, 4/6, 5/6, 6/6, 5/6, 4/6, 3/6, 2/6, 1/6) repeated 100 times to create a 1200-sample time series made up of 100 identical triangular shapes.

Skin-noise amplitude could not be estimated by means of the 3D standard deviation [Eq. (3)] of a node trajectory because the face model was not in a stationary state. Such a standard deviation would contain a skin-noise component and a face-movement component. Fortunately, the results of the previous experiment showed that estimating skin-noise amplitude by means of the difference Δ_{vw} [Eq. (5)] between two node trajectories computed from the same muscle activity but with two different initial conditions or computing precisions led to the same results. Using the difference between two corresponding node trajectories eliminated the face movement component of the 3D standard deviation, leaving only the component of the skin vibration due to the noise.

5.2. Results and discussion. Fig. 4 plots the estimated noise amplitude of the skin model by node number (see Fig. 1b for the approximate position of each node on the face) when the face model was activated by waves of triangular muscle activity. As previously discussed, the amplitudes of the 3D standard deviations were divided by $\sqrt{2}$. To facilitate comparison between the results produced by the face model in the stationary and dynamic states, the thick discontinuous line labeled SShift in Fig. 2 was added to the graph.

The last four lines in Fig. 4 show that using different initial conditions or different computing precisions to estimate noise amplitude did not change the results. A two-way ("node position" and "method" used to estimate noise amplitude) analysis of variance on the noise-amplitude estimates yielded a significant effect of node position [$F(10, 30) = 81.67, p < 1e - 9$] but no significant effect of method [$F(3, 30) = 2.27, p = 0.10$] at the 0.05 level. In other words, skin-noise amplitude was not found to be significantly dependent on computing accuracy or estimator.

A comparison between the thick line labeled SShift and the other four lines in Fig. 4 indicates that the noise amplitude was different, but of the same order of magnitude when the model was in a stationary or dynamic state. A two-way ("node position" and "face-model state") analysis of variance with replication of the noise amplitudes confirmed the significant effect of node position [$F(10, 33) = 87.90p < 1e - 9$], and face-model state [$F(1, 33) = 30.88, p < 1e - 5$], and an interaction between these two factors [$F(10, 33) = 8.81, p < 1e - 6$] at the 0.05 level. However, the similarity of the noise-amplitude estimates produced in the stationary and dynamic states suggests that analogous levels of skin noise may be found in most situations.

6. Experiment 4: Contributions to noise of the muscle and skin models

The muscle models acted as nonlinear modules that processed the electrochemical potentials of the face-model input and interacted with the skin. Both their

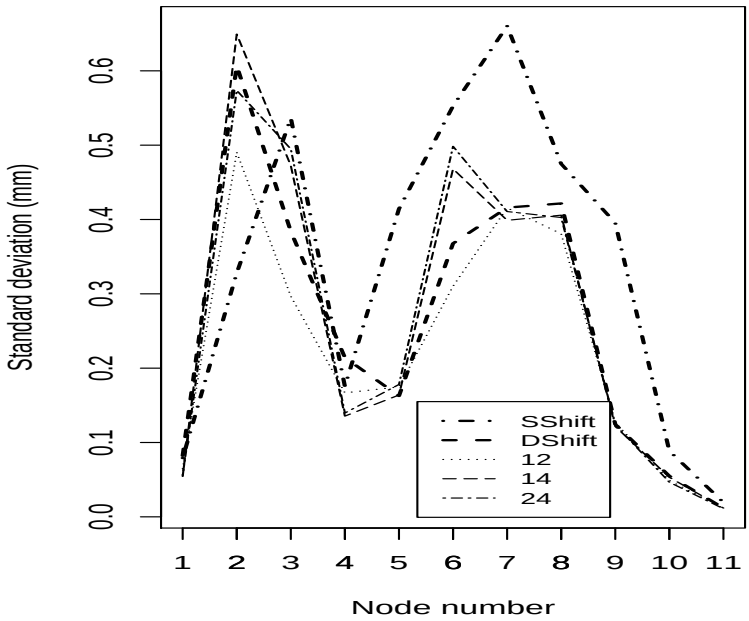

FIGURE 4. Noise-amplitude estimates of the skin model when the modeled muscles were activated by a wave of triangular functions (lines labeled DShift, 12, 14, and 24) or when the face model was in a stationary state (line labeled SShift; data taken from Experiment 2, Fig. 2). DShift means that each node's noise amplitude was estimated by the 3D standard deviation of the difference between two identical animations, except that node 3 was shifted 0.001 mm to the right on the first frame (D stands for Dynamic). The three labels 12, 14, and 24 mean that the standard deviations were estimated by the difference between two identical animations, except that the face model calculations were carried out using two different computing precisions (1 for single, 2 for double, and 4 for quadruple), e.g., 14 for single against quadruple precision.

nonlinear properties and their interactions with the skin could contribute to chaos. Separately analyzing how much of the chaotic noise can be ascribed respectively to the skin model and the muscle model could provide information about which module needs to be improved in order to lower chaotic vibrations. Using the techniques outlined in the first three experiments, the muscle models were checked to make sure that, when separated from the skin model, they did not exhibit chaotic properties , e.g., sensitivity to initial conditions or presence of noise independent of computing accuracy. Then the skin model was analyzed without the muscle models. Since the muscle models did not generate chaotic noise, only the skin analysis will be summarized here.

6.1. Method. The muscle models were replaced by forces proportional to the electrochemical potential used in the previous simulations. The forces were applied to the nodes originally attached to the muscles, in the direction of the lines of action of the discarded muscles. Each force was scaled to the maximum force developed by the corresponding muscle when the muscle was activated by an electrochemical

potential equal to 1. This ensured that the face movements produced would have similar amplitude to those in the previous experiment.

Except for replacing the muscle models by simple forces, this experiment was identical to Experiment 3, i.e., the same wave of 100 triangular shapes was used to activate the skin model, and the noise was computed in the same way.

6.2. Results and discussion. The noise amplitudes were virtually the same as those measured with the muscle models in Experiment 3. The results are therefore not reported here. A two-way ("node position" and "muscle models presence/absence of") yielded a significant effect of node position [$F(10, 66) = 135.92, p < 1e-9$], but not of the muscle-model presence [$F(1, 66) = 0.10, p = 0.75$], and no interaction between these factors [$F(10, 66) = 0.17, p = 0.99$]. Hence, the muscle models did not contribute to the noise analyzed in this paper, and only the skin model was responsible for the results.

7. General discussion

In some applications of nonlinear models, chaotic noise produces an undesirable noise such as soft-tissue vibration. Instead of estimating the Lyapunov exponent of the system, one can directly measure the amplitude of the system's chaotic noise under various conditions. The method proposed here can achieve this goal.

The techniques were tested on a biomechanical model of the face. The results showed that (i) the face model added skin vibration to the facial movements, (ii) the amplitude of the skin noise was approximately equal to 10% of a full-scale movement amplitude and was independent of computing accuracy, i.e., it could not be decreased by improving floating-point precision, (iii) the face model was sensitive to initial conditions, and the results were very similar in the stationary and dynamic states, and (iv) the muscle models did not contribute to skin vibration.

In any application, it must be decided whether the chaotic noise is tolerable or whether it must be decreased. For example, for the face model tested here, chaotic skin vibration was clearly visible in many animations, so decreasing its amplitude was mandatory.

Increasing the damping factors of a dynamic system is a common means of reducing the amplitude of chaotic noise. This solution was not acceptable for the face model because the damping factor increase reduced overly the amplitude of the face movements. I am currently working on how to solve this problem.

A biomechanical model can also be useful in motor control research. The goal of motor control research is to understand how our muscles and articulators are synchronized to achieve a goal such as walking, grasping an object, speaking, etc. A biomechanical model can be used to generate different animations according to several hypothesized motor control strategies. Then perceptual tests can be applied to decide which strategy leads to more natural animations. The impact of chaotic skin vibration on the perceptual results must be assessed to avoid undesirable biases due to chaos.

Determining which muscles of a biomechanical face model must be activated to produce an animation corresponding to a sentence is a difficult problem. Inversions have been proposed in the literature, e.g., [16], [9] or [11]. The principle of these techniques begin by recording the face movements of a real speaker producing the requested corpus and to then apply a mathematical procedure called "inversion" to search in the muscle activity space for a muscle-activity pattern that leads to an animation that matches the recorded movements. No inversions to date have produced inverted muscle activity that matched measurements of real muscle activity.

Hence, determining realistic inverted muscle activity by means of an inversion is still an important challenge in the motor control of speech. This article shows that calculating facial movements from muscle activity adds a non-negligible quantity of skin noise. One can therefore expect to measure similar or worse noise in inversion procedures. As a consequence, inversions should be supplemented by noise analyses to estimate the accuracy limit that can be reached for chaotic noise intrinsic to the biomechanical model. The method presented here (calculating the difference Δ_{vw} [Eq. (5)] between the time series of two inverted muscle-activity levels computed with different initial conditions or computing precisions) can achieve this goal.

Geometrical models of the face are used intensively in the image industry. These models consist of a geometric description of the face surface, often by a mesh of massless points, and a few mathematical parameters that modify the shape of the face in order to generate different expressions and movements [1, 17]. Most facial animations produced in the image industry are based on geometric models because these models are simpler to implement, require less intensive computing, and are easier to control than biomechanical models. However, geometric animations usually look less natural than biomechanical ones. To solve the control problem of a biomechanical model, the dynamic inversion presented in [11] can be used. The results usually seem more natural than anything produced by means of geometric models. The present study showed that chaotic skin vibration must be expected in animations. The method presented here is a simple way of analyzing this skin vibration and may therefore be useful to the image industry.

Acknowledgments

This research was supported by NIH Grant No. DC–00594 from the National Institute of Deafness and other Communication Disorders, and the NSERC. I am grateful to Kevin G. Munhall for his discussion about skin properties and his comments about an earlier draft of this paper. I thank Jorge Lucero for his help regarding the mathematical properties of various ordinary differential equation solvers. I am also grateful to Doug J. K. Mewhort for access to his computers funded by an NSERC equipment grant and by an Academic Equipment Grant from Sun Microsystems of Canada. I extend my thanks to ATR Human Information Processing Research Laboratories, Kyoto, Japan, for granting me access to their morphological data. Finally, I express my gratitude to two anonymous reviewers for their helpful comments.

References

[1] A. Adjoudani, T. Guiard-Marigny, B. Le Goff, L. Reveret, and C. Benoît. A multimedia platform for audio-visual speech processing. In *Eurospeech'97 Proceedings*, volume 3, pages 1671–1674, Rhodes, Greece, 1997. European Speech Communication Association.

[2] P. R. Fenstermacher, H. L. Swinney, and J. P. Gollub. Dynamical instabilities and the transition to chaotic Taylor vortex flow. *Journal of Fluid Mechanics*, 94:103–128, 1979.

[3] M. Geradin, M. Hogge, and G. Robert. Time integration of dynamic equations. In H. Kardestuncer, editor, *Finite Element Handbook*, pages 4.72–4.108. McGraw Hill, 1987.

[4] T. J. R. Hughes. *The Finite Element Method: Linear Static and Dynamic Finite Element Analysis*. Dover Publications, Inc., 2000.

[5] R. Laboissière, D. J. Ostry, and A. G. Feldman. The control of multi-muscle systems: Human jaw and hyoid movements. *Biological Cybernetics*, 74:373–384, 1996.

[6] Y. Lee, D. Terzopoulos, and K. Waters. Realistic modeling for facial animation. In *Proceedings of SIGGRAPH'95 (Computer Graphics Proceedings, Annual Conference Series)*, pages 55–62, Los Angeles, CA, USA, 1995.

[7] E. N. Lorenz. Deterministic nonperiodic flow. *Journal of the Atmospheric Sciences*, 20(2):130–141, 1963.

[8] J. C. Lucero and K. G. Munhall. A model of facial biomechanics for speech production. *The Journal of the Acoustical Society of America*, 106(5):2834–2842, 1999.

[9] S. Morishima, T. Ishikawa, and D. Terzopoulos. Model based 3D facial image reconstruction from frontal image using optical flow. In *ACM SIGGRAPH 98 Conference Abstracts and Applications*, page 258, Orlando, FL, USA, 1998.

[10] Y. Payan, M. Chabanas, X. Pelorson, C. Vilain, P. Levy, V. Luboz, and P. Perrier. Biomechanical models to simulate consequences of maxillofacial surgery. *C. R. Biologies*, 325, 2002.

[11] M. Pitermann and K. G. Munhall. An inverse dynamics approach to face animation. *The Journal of the Acoustical Society of America*, 110(3):1570–1580, 2001.

[12] W. H. Press, S. A. Teukolsky, W. T. Vetterling, and B. P. Flannery. *Numerical Recipes in C*. Cambridge University Press, second edition, 1992.

[13] C. Robert, J. M. Carlson, and J. Doyle. Highly optimized tolerance in epidemic models incorporating local optimization and regrowth. *Physical Review E*, 63(5):Art. no. 056122, 2001.

[14] A. M. Selvam and S. Fadnavis. A superstring theory for fractal spacetime, chaos and quantumlike mechanics in atmospheric flows. *Chaos, Solitons and Fractals*, 10(8):1321–1334, 1999.

[15] D. Terzopoulos and K. Waters. Physically-based facial modeling, analysis, and animation. *The Journal of Visualization and Computer Animation*, 1(2):73–80, 1990.

[16] D. Terzopoulos and K. Waters. Analysis and synthesis of facial image sequences using physical and anatomical models. *IEEE Transactions on Pattern Analysis and Machine Intelligence*, 15(6):569–579, 1993.

[17] E. Vatikiotis-Bateson, T. Kuratate, M. Kamachi, and H. Yehia. Facial deformation parameters for audiovisual synthesis. In *Proceedings of International Conference on Auditory-Visual Speech Processing (AVSP'99)*, pages 118–122, University of California, Santa Cruz, 1999.

[18] K. Waters and D. Terzopoulos. Modeling and animating faces using scanned data. *The Journal of Visualization and Computer Animation*, 2(4):123–128, 1991.

[19] J. M. Winters. Hill-based muscle models: A system engineering perspective. In J. M. Winters and S. Woo, editors, *Multiple Muscle Systems: Biomechanics and Movemement Organization*, pages 69–93. Springer, London, 1990.

[20] F. E. Zajac. Muscle and tendon: properties, models, scaling, and application to biomechanics and motor control. *CRC Critical Reviews in Biomedical Engineering*, 17(4):359–411, 1989.

Laboratoire Parole et Langage, Université de Provence, CNRS, 29 av. Robert Schuman, 13621 Aix-en-Provence cedex, France

E-mail: `michel.pitermann@lpl-aix.fr`